small
NANO MICRO

Fluorographene: A Two-Dimensional Counterpart of Teflon

Rahul R. Nair, Wencai Ren, Rashid Jalil, Ibtsam Riaz, Vasyl G. Kravets, Liam Britnell, Peter Blake, Fredrik Schedin, Alexander S. Mayorov, Shengjun Yuan, Mikhail I. Katsnelson, Hui-Ming Cheng, Wlodek Strupinski, Lyubov G. Bulusheva, Alexander V. Okotrub, Irina V. Grigorieva, Alexander N. Grigorenko, Kostya S. Novoselov,* and Andre K. Geim**

A *stoichiometric derivative of graphene with a fluorine atom attached to each carbon is reported. Raman, optical, structural, micromechanical, and transport studies show that the material is qualitatively different from the known graphene-based nonstoichiometric derivatives. Fluorographene is a high-quality insulator (resistivity >10^{12} Ω) with an optical gap of 3 eV. It inherits the mechanical strength of graphene, exhibiting a Young's modulus of 100 N m^{-1} and sustaining strains of 15%. Fluorographene is inert and stable up to 400 °C even in air, similar to Teflon.*

1. Introduction

Extraordinary properties of graphene continue to attract intense interest that has expanded into research areas beyond the initial studies of graphene's electron transport properties.[1] One of the research directions that have emerged recently is based on the notion of graphene being a giant macromolecule, which as any other molecule can be modified in chemical reactions.[2] Graphene's surface has been decorated with various atoms and molecules[3–7] but stoichiometric derivatives have proven difficult to achieve. There are two known derivatives of graphene: namely, graphene oxide[4] (GO) and graphane.[8] GO is essentially a graphene sheet densely but randomly decorated with hydroxyl and epoxy groups and obtained by exposure of graphite to liquid oxidizing agents. On a microscopic level, GO appears inhomogeneous with a mixture of regions that are pristine and densely decorated.[7] Graphane is a theoretically predicted stoichiometric derivative of graphene with a hydrogen atom attached to each carbon.[8] Graphene membranes with both surfaces exposed to atomic H exhibited a compressed crystal lattice which has served as a proof that this stoichiometric material is realizable.[9] Graphene with only one side exposed to H has a nonstoichiometric composition and, similar to graphene, exhibits metallic conductivity at room temperature (T). Importantly, graphene hydrogenated from either one or both sides rapidly lost H at moderate T,[9] which casts doubts that graphane could be used in applications where stability is required.

One way to create more stable graphene derivatives is to try using agents that bind to carbon stronger than hydrogen. Fluorine is one such candidate and, by analogy with fluorocarbon, we refer to fully fluorinated graphene as fluorographene

R. R. Nair, R. Jalil, I. Riaz, Dr. V. G. Kravets, L. Britnell, Dr. P. Blake, Dr. F. Schedin, Dr. A. S. Mayorov, Dr. I. V. Grigorieva, Dr. A. N. Grigorenko, Prof. K. S. Novoselov, Prof. A. K. Geim,
School of Physics and Astronomy
University of Manchester
Manchester, M13 9PL, U.K
E-mail: rahul.raveendran-nair@postgrad.manchester.ac.uk; kostya@manchester.ac.uk; geim@manchester.ac.uk

Dr. W. C. Ren, Prof. H. M. Cheng
Shenyang National Laboratory for Materials Science
Institute of Metal Research
Chinese Academy of Sciences
72 Wenhua Road, Shenyang 110016, P. R. China

Dr. S. Yuan, Prof. M. I. Katsnelson
Radboud University of Nijmegen
Institute for Molecules and Materials
Nijmegen, 6525 AD, The Netherlands

Prof. W. Strupinski
Institute of Electronic Materials Technology
Wólczyńska 133, Warszawa 01–919, Poland

Dr. L. G. Bulusheva, Prof. A. V. Okotrub
Nikolaev Institute of Inorganic Chemistry
SB RAS, 630060 Novosibirsk, Russia

DOI: 10.1002/smll.201001555

(FG). FG is a two-dimensional (2D) analogue of Teflon, which is a fully fluorinated (FF) 1D carbon chain. Alternatively, one can consider FG as a 2D counterpart of graphite fluoride (GrF), a 3D compound used in batteries and as a lubricant.[10] Recently, mechanical cleavage[11] was attempted to extract individual atomic planes (i.e., FG) from commercially available GrF, but it proved surprisingly difficult, and only multilayered samples were reported.[12–14] Moreover, the studied multilayers exhibited electronic and Raman properties that, as shown below, resemble partially reduced FG and are qualitatively different from the stoichiometric material reported here. The latter is a wide-gap insulator with a mechanical strength and elasticity similar to graphene, and a thermal stability and chemical inertness matching those of Teflon. The 2D insulator complements metallic properties offered by its parent material and can be used as a atomically thin tunnel barrier.

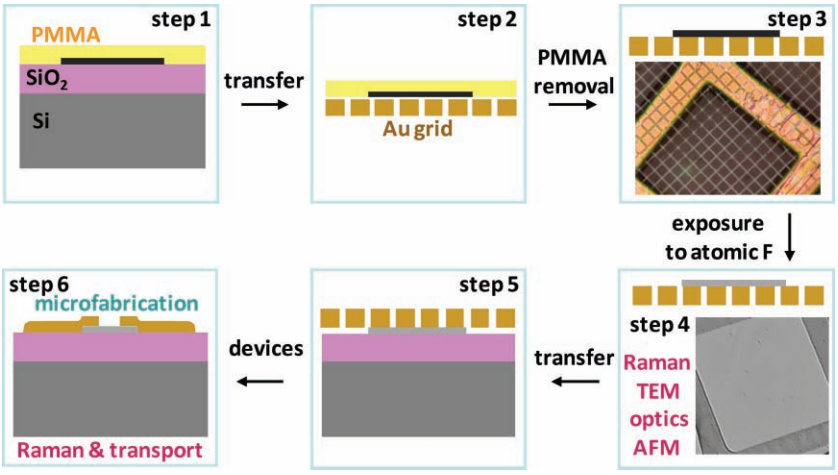

Figure 1. Various steps involved in our investigation. They are discussed in detail in the Experimental Section. PMMA - poly(methyl methacrylate.)

2. Results and Discussion

2.1. From Graphene to Fluorographene

We have employed two complementary approaches for obtaining FG. One is the mechanical cleavage of GrF, similar to other reports.[12–14] Its monolayers were found to be extremely fragile and prone to rupture, due to many structural defects resulting from the harsh fluorination conditions used to obtain bulk GrF.[10,15] Nevertheless, we have succeeded in extracting GrF monolayers of ~1 μm in size (see Supporting Information, Section #1) and used them in Raman studies. To prepare large FG samples suitable for most of our experiments, we have found it both necessary and convenient to employ an alternative approach in which graphene was exposed to atomic F formed by decomposition of xenon difluoride (XeF_2)[16] (note that, at room T, graphene is stable in molecular F_2).[10] This approach has a clear advantage with respect to possible fluorination in plasma (as employed for hydrogenation of graphene)[9] because the use of XeF_2 avoids a potential damage due to ion bombardment. Furthermore, fluorination by XeF_2 is a simple low-hazard procedure that can be implemented in any laboratory.

The processing chart to obtain FG samples used in our experiments is shown in **Figure 1**. In brief, we prepared large graphene crystals (>100 μm in size) by using the standard cleavage technique.[11] Because XeF_2 rapidly etches Si and easily diffuses through even a thick layer of amorphous SiO_2, it appeared impossible to use Si wafers in the fluorination procedures. Keeping in mind the necessity of using a chemically inert support and the fact that complete fluorination requires the exposure of graphene from both sides, we transferred the cleaved crystals onto Au grids used for transmission electron microscopy (TEM). To provide sufficient support for graphene, we used Au grids covered with Quantifoil, a lithographically patterned polymer film (see Figure 1). The samples were then placed in a Teflon container with XeF_2 and heated to 70 °C (the elevated T speeded up the reaction; the use of even higher T destroyed the Au grids). The resulting samples were then used for Raman, TEM, and optical studies and probed by atomic force microscopy (AFM). For electrical characterization, FG was transferred from TEM grids back onto an oxidized Si wafer. The latter was done by pressing the grids against the wafer or by using the capillary transfer method.[17]

2.2. Raman Spectroscopy of Fluorinated Graphene

The evolution of graphene's Raman spectra due to its consecutive exposures to atomic F is shown in **Figure 2**. One can see that first a prominent **D** peak emerges. This indicates the appearance of atomic scale defects.[18,19] As the fluorination time increases, the double-resonance band (usually referred to as **2D** or **G'** peak) disappears whereas **D** and **G** peak intensities remain approximately the same (Figure 2b). With increasing fluorination time (a few days), all the Raman features gradually disappear. This behavior is radically different from that observed for hydrogenated graphene, in which case the **2D** band always remains strong.[9] Partially fluorinated graphene (10–20 h) exhibits the Raman spectra that resemble those of GO, which also has comparable intensities of the **G** and **D** peaks and a relatively small **2D** band.[7,20] The disappearance of all the characteristic peaks clearly proves more dramatic changes induced by fluorination in comparison with those reported for hydrogenated graphene and GO. We explain this by complete optical transparency of FF graphene to our green laser light. Indeed, according to theory,[21,22] GrF should have an energy gap of $E_g \approx 3.5$ eV (the gap has not been measured previously,[10] probably because the material usually comes in the form of an opaque white powder).

It is instructive to compare the observed spectrum of FG with Raman spectra of bulk GrF and a monolayer extracted

NANO MICRO small

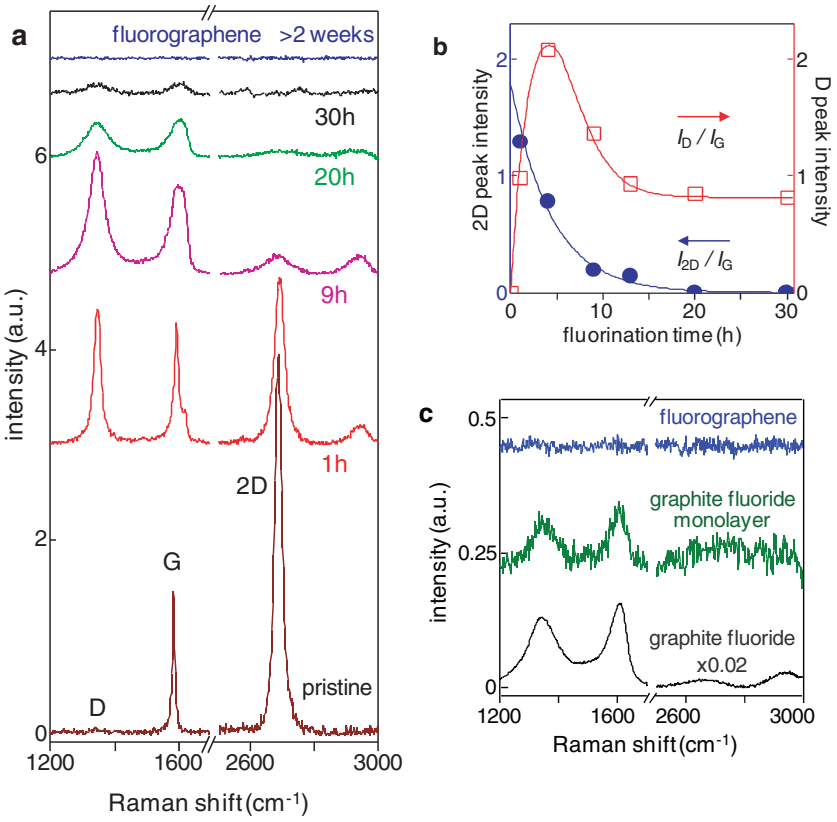

Figure 2. Raman signatures of FG. a) Evolution of the spectra for a graphene membrane exposed to atomic F and measured each time under the same Raman conditions. The curves are shifted for clarity. b) Intensities of the **D** and **2D** peaks (normalized with respect to the **G** peak intensity) as a function of fluorination time. Solid curves are guides to the eye. c) Comparison of our FF membranes with GrF and its monolayer. The measurements were done under the same conditions. The curves are shifted for clarity, and the one for bulk GrF is scaled down by a factor of 50. For strongly fluorinated samples, a smooth background due to luminescence was removed.

from the latter (Figure 2c). One can see that, within the noise level, the latter two are identical and correspond to the spectrum of partially fluorinated graphene (close to the state achieved after 20–30 h in Figure 2a). This is surprising because GrF normally exhibits fluorine-to-carbon ratios larger than unity (in our case, the ratio is ≈1.1; see Supporting Information) and is assumed to be fully fluorinated.[10] The nonstoichiometric F:C ratios are due to the presence of numerous structural defects that allow more C bonds to be terminated with fluorine (CF_2 and CF_3 bonding). Our Raman data show that, despite F:C > 1, GrF planes remain not fully fluorinated, and one should not use GrF spectra as a reference to achieve a FF state.

2.3. Structure and Stability

Structural information about FG was obtained by TEM. **Figure 3**a shows an electron diffraction image for a FF membrane. The image yields a perfect hexagonal symmetry and is similar in quality to those observed for pristine graphene.[23] The unit cell of FG is slightly expanded with respect to graphene's cell, in contrast to the case of hydrogenated graphene that showed a compressed lattice.[9] FG's lattice was found to be the same for all the studied FF membranes, and its expansion was isotropic (no axial strain was observed).[9] Figure 3b shows histograms for the lattice constant d in graphene and FG. The spread in the recorded values is due to a limited accuracy of TEM in precision measurements of d. Nonetheless, one can clearly see that FG has a unit cell approximately 1% larger than graphene, that is, $d \approx 2.48$ Å. An increase in d is expected because fluorination leads to sp^3-type bonding that corresponds to a larger interatomic distance than sp^2. However, the observed increase is smaller than that in GrF, where d values were reported to be 2.8–4.5% larger than those in graphite.[15,24] The smaller d in FG is probably due to the possibility for the 2D sheet to undergo strong interatomic corrugations if out-of-plane displacements of carbon atoms are not restricted by the surrounding 3D matrix, similar to the case of graphane which is predicted[8] to have a d value close to the one we observed for FG.

The Raman signatures for complete and partial fluorination in Figure 2a allowed us to study the FG stability at elevated T and with respect to exposure to various chemicals (also, see Supporting Information, Section #3). For graphene fluorinated only for a few hours, the process was found to be largely reversible, so that a short annealing at 250 °C in an argon–hydrogen mixture (10% H_2) could restore membranes to their nearly pristine state, showing only a small remaining **D** peak in their spectra. After more extensive fluorination (>20 h), annealing even at 450 °C could not restore the **2D** peak, but the **D** and **G** peaks notably grew and became similar in intensity to those on, for example, the 9 h curve in Figure 2a, which indicates that a significant amount of F remained attached to the carbon scaffold. For FF graphene, its Raman spectra did not change for T up to 200 °C and losses of F became discernable only for prolonged annealing above 400 °C.

FG was also found to be stable in such liquids as water, acetone, and propanol, and under ambient conditions. The chemical stability is similar to that of graphite fluoride and Teflon, although our tests were not exhaustive. Note that we have also investigated digraphite fluoride (C_2F), a stage II intercalation graphite compound.[25] This material allowed relatively easy exfoliation, but was unstable in any of the above liquids. Its single- and few-layer crystals were unstable even under ambient conditions, reducing rapidly to the state similar to strongly damaged graphene or reduced GO. Further information about FG's stability was obtained in transport experiments discussed below.

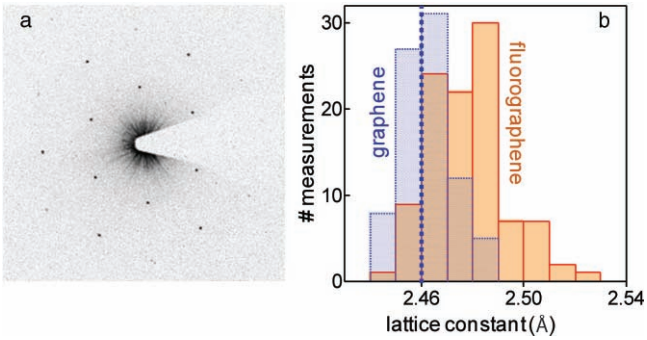

Figure 3. Transmission electron microscopy of FG. a) Diffraction pattern from a FG membrane. b) Lattice constant *d* measured using microscopy images, such as that shown in (a). For comparison, similar measurements were taken for membranes before fluorination (left histogram). The dotted line indicates *d* for graphite.

2.4. Optical Properties

The absence of Raman signatures for FG has indicated its optical transparency. **Figure 4** extends this qualitative observation by showing absorption spectra of pristine, partially fluorinated, and FF graphene. The measurements were done for graphene deposited onto quartz wafers and then fluorinated in XeF_2 at 70 °C, which did not damage quartz in a moisture-free atmosphere. This method allowed us to obtain large crystals (>100 μm in size) suitable for standard optical spectroscopy. The crystals' transparency was measured with respect to the wafer.

The upper curve in Figure 4 is for pristine graphene. For light energies $E < 2.5$ eV, it exhibits a flat absorption spectrum $abs(E)$ with a "universal opacity" of $\pi\alpha \approx 2.3\%$ where α is the fine structure constant.[26,27] Strong deviations from this universality take place in blue light, and graphene's opacity triples in peak intensity at 4.6 eV. This is due to the fact that graphene's spectrum is no longer linear at energies close to the hopping energy of ~2.5 eV and exhibits a pronounced van Hove singularity.[28–30] Note that the peak is clearly asymmetric with a low-E tail, which is attributed to excitonic effects.[29,30]

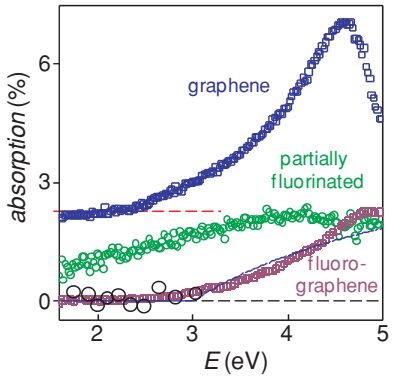

Figure 4. Changes in optical transparency of graphene due to fluorination. The upper curve is for graphene and, within experimental error, follows the low-*E* data of reference [26]. Beyond the previously reported range (<3 eV), graphene exhibits an absorption peak in the ultraviolet range. Partially fluorinated graphene shows higher transparency (middle curve). FG is transparent for $E \leq 3$ eV, but starts absorbing violet light. The large open circles are the measurements for FG membranes on a TEM grid using filter spectroscopy.[26] The dashed lines indicate zero and $\pi\alpha$ opacities. The solid curve is the absorption behavior expected for a 2D semiconductor with $E_g = 3$ eV.

For graphene fluorinated on quartz, its state was first assessed by Raman spectroscopy. Although F should be able to diffuse between graphene and quartz,[10] the concentration of atomic F underneath the graphene sheet is probably limited by its recombination into less reactive F_2. Accordingly, it required several days to reach the fluorination state similar to that achieved after 9 h for membranes in Figure 2a. The partially fluorinated graphene exhibited enhanced transparency with respect to graphene over the whole E range (Figure 4) and, for visible light, its opacity fell down to ~0.5%. Because impurity scattering is not expected to result in any significant decrease in optical conductivity, the enhanced transparency of the partially fluorinated state can only be explained by a gap that opens in graphene's electronic spectrum (Supporting Information, Section #7). The remnant absorption can be attributed to microscopic regions that remain nonfluorinated, similar to the case of GO.[7]

After several weeks of fluorination, we achieved the Raman state that corresponded to the 30 h curve in Figure 2a. This highly fluorinated state was found to be transparent at visible frequencies and started absorbing light only in the blue range (Figure 4). This proves that FG is a wide-gap semiconductor with $E_g \geq 3.0$ eV. To confirm this result, we also used the technique described in reference [26], which analyzed images obtained in an optical microscope by using a set of narrow-pass filters. The latter approach limited our measurements to the visible spectrum, but allowed the use of FF membranes directly on a TEM grid. No opacity was detected for these samples at all frequencies accessible by the microscopy approach (large symbols in Figure 4).

Unlike bulk semiconductors, 2D materials remain partially transparent even at E above the energy gap. The analysis given in reference [30] can be extended for a 2D semiconductor with a parabolic spectrum and yields $abs(E) \approx 2\pi\alpha(1 - E_g/E)$ for $E \geq E_g$. This dependence is shown by the solid curve in Figure 4. For a gapped Dirac spectrum, we find $abs(E) \approx \pi\alpha(1 - E_g^2/E^2)$, which fits the experimental data equally well, but probably is less appropriate for the graphene spectrum with such a large gap. The measured spectra could also be influenced by excitonic effects, and thus, provide the lower bound for the real bandgap of FG; therefore, we refer to the observed cut-off as an optical gap.

2.5. Insulating Properties

To assess the electrical properties of FG, we transferred our samples from Quantifoil onto an oxidized Si wafer and made multiterminal devices, such as that shown in **Figure 5**. Even weakly fluorinated graphene (with Raman spectra similar to the 1 h curve in Figure 2a) was found to be highly insulating, exhibiting room-T resistivity ρ in the MΩ range, that is, three orders of magnitude higher than graphene (Supporting

small NANO MICRO

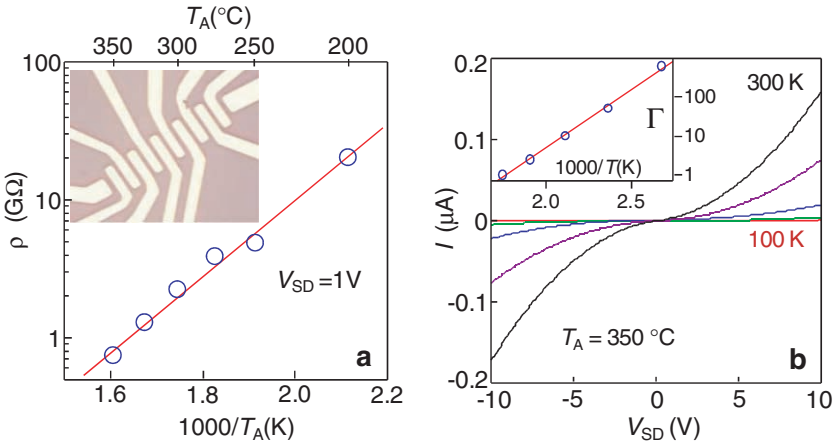

Figure 5. Highly stable 2D insulator. a) Changes in FG's ρ induced by annealing. No changes could be detected at T_A below 200 °C. At higher T_A, ρ falls below 1 TΩ and becomes measurable in our experiments. Because of nonlinear *I–V* characteristics, the plotted ρ values were recorded for a fixed bias V_{SD} of 1 V (circles). For any given T_A, we found that it required approximately 1 h to reach a saturated state. The solid line is the exponential dependence yielding $E_{des} \approx 0.65$ eV. The inset shows one of our devices with the distance between adjacent contacts of 2 μm. b) *I–V* characteristics for partially fluorinated graphene obtained by reduction at 350 °C. The curves from flattest to steepest were measured at $T = 100$, 150, 200, 250, and 300 K, respectively. The scaling factor Γ is plotted in the inset. The solid line is the best fit by $\exp(E_h/T)$.

Information, Section #5). This clearly distinguishes fluorination from hydrogenation, with the latter resulting in little increase in ρ at room T.[9] The devices made from FF graphene showed no leakage current at biases V_{SD} up to 10 V (within our detection limit of ~0.1 nA due to parasitic conductivities; Supporting Information, Section #5). Taking into account that the devices had typical width-to-length ratios of 10–100, this sets a lower limit on FG's ρ of $>10^{12}$ Ω at room T. Such a highly insulating state is in agreement with the presence of a wide bandgap.

Electrical measurements allowed us to study thermal stability of FG in more detail than the Raman spectroscopy. Figure 5a shows changes in electrical conductivity induced by annealing at different temperature T_A in the argon–hydrogen atmosphere. No current could be detected through FG after its prolonged annealing at T_A below 200 °C. At higher T_A, FG became weakly conductive (see Figure 5a), and at T as high as 350 °C its effective resistivity $\rho = V/I$ fell down to ~1 GΩ if we applied a large source–drain voltage V_{SD} of 1 V. This behavior is in agreement with the changes observed in Raman spectra due to annealing (see above and Supporting Information, Section #3). The $\rho(T_A)$ dependence in Figure 5a is well described by the functional form $\exp(E_{des}/T_A)$ with desorption energy $E_{des} \approx 0.65$ eV. The found E_{des} is notably lower than the C–F bond energy of ~5.3 eV, indicating that the initial desorption occurs from defective sites. This is consistent with the studies of GrF, which show that its decomposition is initiated at structural defects and strained regions.[31] The defect-mediated desorption is also supported by the fact that saturated states in Figure 5a are rapidly achieved after <1 h of annealing and no further changes occur for longer exposures to a given T_A.

The electrical measurements of devices partially reduced by annealing also confirm that the material is a wide-bandgap insulator, in agreement with our Raman and optical measurements. To this end, we measured *I–V* characteristics of FG strongly reduced at 350 °C (Figure 5b). They collapse on a single *I–V* curve if scaled along the *I* axis (not shown). The found prefactor Γ is plotted in the inset. The T dependence of Γ is well described by the activation dependence $\exp(E_h/T)$ with $E_h \approx 0.6$ eV. The value is smaller than the minimum activation energy $E_g/2 \approx 1.5$ eV expected from our optical studies. This implies a broad band of impurity states inside the gap, which can be attributed to fluorine vacancies, which appear during annealing. In this case, electron transport occurs via activation from the impurity band to the conduction or valance band, the mechanism common for semiconductors with a high density of deep dopants.[32] In the FF state (before annealing), E_h should be significantly higher, but we could not observe any conductivity for FG to estimate its transport gap.

We emphasize that the thermal stability of FG is higher than that of graphene, GO, and even GrF. Under the same conditions, GrF starts decomposing already at 300 °C.[31] The higher stability of FG can be attributed to the absence of structural defects and little strain. As for Teflon, it undergoes slow decomposition at $T >$ 260 °C and rapidly decomposes only above 400 °C.[33] Our transport measurements are sensitive to minor compositional changes (indicating none below ~200 °C) while the Raman spectra discussed above revealed notable F losses only above 400 °C (Supporting Information, Section #3). These characteristics are very similar to those of Teflon.[33]

2.6. Stiffness and Mechanical Strength

GrF contains many structural defects induced by fluorination procedures.[10,15] If our FG were similarly fragile, this would severely limit its possible applications. To gain information about the mechanical properties of FG, we have employed AFM. Quantifoil with a periodic array of circular apertures was used as a supporting scaffold (see the AFM image in **Figure 6**a, inset). The experimental arrangements and analysis were similar to those of reference [34] (Supporting Information #6). In brief, an AFM tip was positioned above the center of a FG membrane and then moved down to indent it. We recorded the bending of the AFM cantilever as a function of its displacement, and the force acting on the membrane was calculated from the cantilever's rigidity.[34,35] Figure 6a shows typical loading curves. As a reference, we used pristine graphene on identical Quantifoil grids. This allowed us to crosscheck the results and avoid systematic errors due to finite rigidity of the polymer scaffold, which also responded to the load. Our analysis of the force-displacement curves has yielded Young's modulus E of FG $\approx 100 \pm 30$ N m^{-1} or 0.3 TPa,[34] that is, FG is 3 times less stiff than graphene.

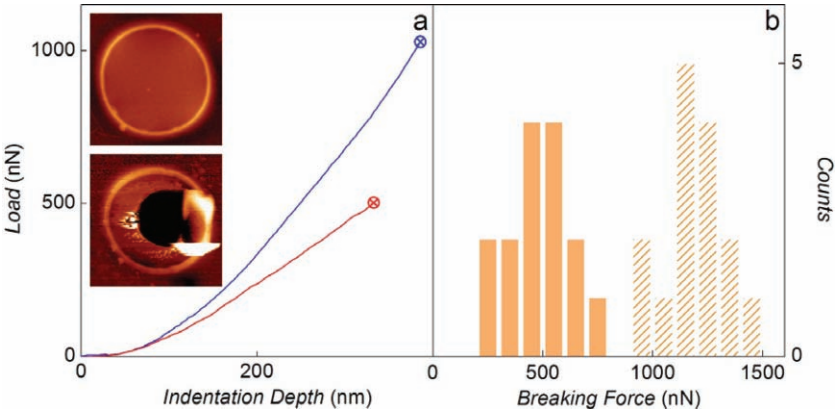

Figure 6. Mechanical properties of FG. a) Examples of the loading curves for graphene (blue) and FG (red) membranes. Fracture loads are marked by the circled crosses. Until these breaking points, the curves were nonhysteretic. Top and bottom insets: AFM images of a FG membrane before and after its fracture, respectively. The lateral scale for the images is given by their width of 2.2 μm; *Z*-scale is approximately 100 nm. b) Histogram for the breaking force for graphene (hashed) and FG (solid color). All the membranes (15 of each type) were on identical Quantifoils and punched by the same AFM tip.

To measure FG's breaking strength, we indented the membranes until they collapsed (Figure 6a). The observed values for the breaking force are collected in Figure 6b. Both graphene and FG show similar histograms, but graphene exhibits on average ~2.5 times higher strength. This infers FG's intrinsic strength $\sigma \approx 15$ N m^{-1}. This reduction in stiffness and breaking strength is generally expected due to the longer sp^3-type bonding in FG. Nonetheless, we emphasize that both E and σ are extremely high in comparison with other materials (e.g., structural steel). What's more, graphene and FG can sustain the same elastic deformations σ/E of ~15%. This can be readily seen from Figure 6a where both membranes broke at similar indentations. The large breaking strength of FG and the fact that it supports such high strains prove its minimal damage during fluorination and the practical absence of structural defects.

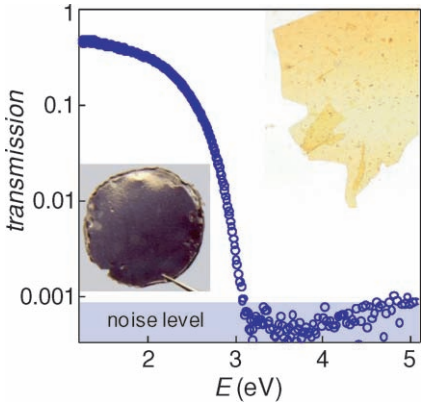

Figure 7. Graphene paper before and after fluorination (left and right insets, respectively). The plot shows optical transparency of FG paper as a function of *E* for a 5 μm thick sample in the photo. The FG sample size is approximately 1 cm.

2.7. Fluorographene Paper: 2D Teflon

To demonstrate that it is possible to scale up the production of FG for applications, we have fluorinated graphene laminates and graphene on SiC. Laminates were obtained by filter deposition from a graphene suspension that was prepared by sonication of graphite.[36,37] To speed up the fluorination process that involves diffusion of F between crystallites, we exposed the laminate to XeF_2 at 200 °C. A period of 10 h was sufficient to reach a saturated state that did not change with further fluorination. Note that, under the same conditions, graphite could not be fluorinated (higher T values are employed to produce GrF[10]). This implies that multilayer graphene present in laminates[36,37] probably remains not FF (Supporting Information, Section #2). Graphene on SiC is discussed in Supporting Information, Section #4.

Figure 7 shows optical photographs of a graphene laminate before and after its fluorination. The resulting material is visually distinctive from the original, which is completely black with metallic shine (see the left inset of Figure 7). In contrast, FG paper is transparent and has a yellowish color that corresponds to absorption in violet (right inset). This is direct visual proof that FG is a wide-gap material. Its optical spectrum is also shown in Figure 7. The light transmission exhibits an onset at ~3.1 eV, in agreement with the gap value inferred from the absorption spectra of individual FG crystals. The smaller gap with respect to GrF predicted to have $E_g \approx 3.5$ eV[21,22] or higher can be due to an atomically corrugated structure or excitonic effects. Note that GO has a color somewhat similar to FG, but the former absorbs much more light and GO paper becomes completely nontransparent already at sub-micrometer thicknesses. Furthermore, the spectrum in Figure 7 is qualitatively different from that of GO, which shows no apparent gap.[7] FG paper is strongly hydrophobic (similar to GrF) and stable under ambient conditions and at elevated T as expected from our studies of individual FG crystals.

3. Conclusion

We have shown that the exposure of graphene to atomic F results in a stoichiometric derivative that is an excellent insulator with high thermal and chemical stability. The optical and electrical properties of FG are radically different from those of graphene, graphene oxide and hydrogenated graphene due to a wide gap opened in the electronic spectrum. Mechanically, FG is remarkably stiff but stretchable, similar to its record-breaking parent, graphene. These characteristics rival those of Teflon and allow one to consider FG for a range of technologies, in particular those that employ Teflon rather than GrF or require better inertness and stability than unachievable for the latter compound. As for electronic applications, particularly promising seems the possibility to

small NANO MICRO

use FG as an atomically thin insulator or a tunnel barrier in graphene-based heterostructures such as, for example, the widely discussed graphene double layers, which have to be electrically decoupled by an atomically thin insulator. More generally, FG adds to the small family of graphene-based derivatives that previously consisted of only GO and hydrogenated graphene.

Note Added at Proof: Related results were published online[38] three months after our initial submission of this manuscript. During this period, papers in references [12–14] were also published. As they were previously available online, we were able to discuss them in the Introduction. As for the latest report,[38] it deals with graphene films grown on Cu and fluorinated using XeF_2 at room *T*. The authors refer to their material as perfluorographane. It is a nonstoichiometric compound with a significant amount of fluorine adsorbed onto structural defects, which involves C–F_2, C–F_3, and other types of bonding as follows from the reported X-ray photoelectron spectroscopy data. This leaves many carbon sites within the graphene sheet itself nonfluorinated. The insulating and Raman properties of perfluorographane show behavior similar to our samples of partially fluorinated graphene (approximately 30 h in Figure 2), and we reach similar conclusions about these properties (see section 2.2 and 2.5 above and Supporting Information). The optical gap observed in our experiment is in agreement with the calculations presented in reference [38].

4. Experimental Section

Fluorination: Large graphene crystals were prepared on top of an oxidized silicon wafer (300 nm of SiO_2) by using micromechanical cleavage. Because of high reactivity of Si with atomic fluorine, we had to transfer graphene onto gold and nickel grids that could sustain the fluorination procedures. This approach also allowed us to expose graphene to F from both sides. As the first step (see Figure 1), a thin polymer layer (100 nm of PMMA) was deposited on top of the wafer with graphene crystals. The PMMA film provided a mechanical support for graphene during further processing. Then, the SiO_2 layer was etched away in 3% potassium hydroxide solution, which lifted off the PMMA film together with graphene crystals. After thorough cleaning in deionized water, the film floating in water was picked up onto a TEM grid (step 2 in Figure 1). Finally, PMMA was dissolved in acetone, and the samples were dried using a critical point dryer. The optical micrograph in Figure 1 (step 3) shows one of our Quantifoil-Au grids. The size of the Quantifoil mesh is 7 μm, and graphene covers the whole Au cell. Graphene membranes on Quantifoil were then exposed to XeF_2 at 70 °C (~1 g in a 3 mL PTFE (polytetrafluoroethylene) container). The procedure was carried out in a glovebox to avoid any moisture that could result in the formation of HF. The TEM image in Figure 1 (step 4) shows one of the Quantifoil cells fully covered with FG. Its presence can be witnessed as small dust particles within the aperture. We also fluorinated graphene crystals cleaved on top of quartz wafers. Such samples were used for the optical spectroscopy measurements.

Increasing the Speed of Fluorination: We have found that it is possible to significantly increase the speed by using higher *T*. To this end, a PTFE-lined stainless steel container (Parr Instruments) was used. The high-*T* procedure required graphene to be placed on Ni grids that, unlike gold, could sustain XeF_2 at 200 °C. Using this approach, the FF state could be reached within a few hours rather than weeks. In our report above, it was more instructive to show gradual changes from graphene to fluorographene, which were easier to follow using the low *T* fluorination. The use of higher *T* is important for applications, and also this proves that the FF state discussed above was final. Indeed, prolonged fluorination at 200 °C led to the same Raman, optical, and transport characteristics as those achieved for very long exposures at 70 °C.

Further Experimental Details: The Raman studies were carried out using a Renishaw spectrometer with a green (514 nm) laser. For optical spectroscopy experiments, we used a xenon lamp (250–1200 nm) and an Ocean Optics HR2000 spectrometer. A Tecnai F30 TEM instrument operated at 300 kV was employed for studies of the FG's structure. For micromechanical measurements, we used a MultiMode Nanoscope (Veeco) and, for electrical measurements, FG was transferred from a TEM grid back onto an oxidized Si wafer (step 5 in Figure 1). The standard microfabrication procedures[1,11] including electron beam lithography were then employed to make electrical contacts (step 6). More details are provided in the Supporting Information.

Supporting Information

Supporting Information is available from the Wiley Online Library or from the author.

Acknowledgements

The work was supported by the Office of Naval Research, EPSRC (UK), the Körber Foundation, the Air Force Office of Scientific Research and the Royal Society. W. C. Ren acknowledges the support from CAS and NSFC.

[1] A. K. Geim, K. S. Novoselov, *Nat. Mater.* **2007**, *6*, 183.
[2] R. Ruoff, *Nat. Nanotechnol.* **2008**, *3*, 10.
[3] F. Schedin, A. K. Geim, S. V. Morozov, E. W. Hill, P. Blake, M. I. Katsnelson, K. S. Novoselov, *Nat. Mater.* **2007**, *6*, 652.
[4] S. Park, R. S. Ruoff, *Nat. Nanotechnol.* **2009**, *4*, 217.
[5] H. Liu, S. Ryu, Z. Chen, M. L. Steigerwald, C. Nuckolls, L. E. Brus, *J. Am. Chem. Soc.* **2009**, *131*, 17099.
[6] R. Sharma, J. H. Baik, C. J. Perera, M. S. Strano, *Nano Lett.* **2010**, *10*, 398.
[7] G. Eda, M. Chhowalla, *Adv. Mater.* **2010**, *22*, 2392.
[8] J. O Sofo, A. S. Chaudhari, G.D. Barber, *Phys. Rev. B* **2007**, *75*, 153401.
[9] D. C. Elias, R. R. Nair, T. M. G. Mohiuddin, S. V. Morozov, P. Blake, M. P. Halsall, A. C. Ferrari, D. W. Boukhvalov, M. I. Katsnelson, A. K. Geim, K. S. Novoselov, *Science* **2009**, *323*, 610.
[10] N. Watanabe, T. Nakajima, H. Touhara, *Graphite Fluorides*, Elsevier, Amsterdam **1988**.
[11] K. S. Novoselov, D. Jiang, F. Schedin, T. J. Booth, V. V. Khotkevich, S. V Morozov, A. K. Geim, *Proc. Natl. Acad. Sci. USA* **2005**, *102*, 10451.

[12] K. A Worsley, P. Ramesh, S. K. Mandal, S. Niyogi, M. E. Itkis, R. C. Haddon, *Chem. Phys. Lett.* **2007**, *445*, 51.
[13] S. H. Cheng, K. Zou, F. Okino, H. R. Gutierrez, A. Gupta, N. Shen, P. C. Eklund, J. O. Sofo, J. Zhu , *Phys. Rev. B* **2010**, *81*, 205435.
[14] F. Withers, M. Dubois, A. K. Savchenko, arxiv:1005.3474, **2010**.
[15] Y. Kita, N. Watanabe, Y. Fujii, *J. Am. Chem. Soc.* **1979**, *101*, 3832.
[16] U. Dettlaff-Weglikowska, V. Skakalova, J. Meyer, J. Cech, B. G. Mueller, S. Roth, *Curr. Appl. Phys.* **2007**, *7*, 42.
[17] J. C. Meyer, C. O. Girit, M. F. Crommie, A. Zettl, *Appl. Phys. Lett.* **2008**, *92*, 123110.
[18] A. C. Ferrari, *Solid State Commun.* **2007**, *143*, 47.
[19] L. M. Malard, M. A. Pimenta, G. Dresselhaus, M. S. Dresselhaus, *Phys. Rep.* **2009**, *473*, 51.
[20] D. Yang, A. Velamakanni, G. Bozoklu, S. Park, M. Stoller, R. D. Piner, S. Stankovich, I. Jung, D. A. Field, C. A. Ventrice, R. S. Ruoff, *Carbon* **2009**, *47*, 145.
[21] J. C. Charlier, X. Gonze, J. P. Michenaud, *Phys. Rev. B* **1993**, *47*, 16162.
[22] Y. Takagi, K. Kusakabe, *Phys. Rev. B* **2002**, *65*, 121103.
[23] J. C. Meyer, A. K. Geim, M. I. Katsnelson, K. S. Novoselov, T. J. Booth, S. Roth, *Nature* **2007**, *446*, 60.
[24] H. Touhara, K. Kadono, Y. Fujii, N. Watanabe, Z. *Anorg. Allg. Chem.* **1987**, *544*, 7.
[25] A. V. Okotrub, I. P. Asanov, N. F. Yudanov, K. S. Babin, A. V. Gusel'nikov, T. I. Nedoseikina, P. N. Gevko, L. G. Bulusheva, Z. Osvath, L. P. Biro, *Phys. Status Solidi B* **2009**, *246*, 2545.
[26] R. R. Nair, P. Blake, A. N. Grigorenko, K. S. Novoselov, T. J. Booth, T. Stauber, N. M. R. Peres, A. K. Geim, *Science* **2008**, *320*, 1308.
[27] K. F. Mak, M. Y. Sfeir, Y. Wu, C. H. Lui, J. A. Misewich, T. F. Heinz, *Phys. Rev. Lett.* **2008**, *101*, 196405.
[28] T. Stauber, N. M. R. Peres, A. K. Geim, *Phys. Rev. B* **2008**, *78*, 085432.
[29] L. Yang, J. Deslippe, C. H. Park, M. L. Cohen, S. G. Louie, *Phys. Rev. Lett.* **2009**, *103*, 186802.
[30] V. G. Kravets, A. N. Grigorenko, R. R. Nair, P. Blake, S. Anissimova, K. S. Novoselov, A. K. Geim, *Phys. Rev. B* **2010**, *81*, 155413.
[31] N. Kumagai, M. Kawamura, H. Hirohata, K. Tanno, Y. Chong, N. Watanabe, J. *Appl. Electrochem.* **1995**, *25*, 869.
[32] B. I. Shklovskii, A. L. Efros, *Electronic Properties of Doped Semiconductors*, Springer, Berlin **1984**.
[33] J. A. Conesa, R. Font, *Polym. Eng. Sci.* **2001**, *41*, 2137.
[34] C. Lee, X. D. Wei, J. W. Kysar, J. Hone, *Science* **2008**, *321*, 385.
[35] M. Poot, H. S. J. Van Der Zant, *Appl. Phys. Lett.* **2008**, *92*, 063111.
[36] Y. Hernandez, V. Nicolosi, M. Lotya, F. M. Blighe, Z. Sun, S. De, I. T. McGovern, B. Holland, M. Byrne, Y. K. Gun'Ko, J. J. Boland, P. Niraj, G. Duesberg, S. Krishnamurthy, R. Goodhue, J. Hutchison, V. Scardaci, A. C. Ferrari, J. N. Coleman, *Nat. Nanotechnol.* **2008**, *3*, 563.
[37] P. Blake, P. D. Brimicombe, R. R. Nair, T. J. Booth, D. Jiang, F. Schedin, L. A. Ponomarenko, S. V. Morozov, H. F. Gleeson, E. W. Hill, A. K. Geim, K. S. Novoselov, *Nano Lett.* **2008**, *8*, 1704.
[38] J. T. Robinson, J. S. Burgess, C. E. Junkermeier, S. C. Badescu, T. L. Reinecke, F. K. Perkins, M. K. Zalalutdniov, J. W. Baldwin, J. C. Culbertson, P. E. Sheehan, E. S. Snow, *Nano Lett.* **2010**, *10*, 3001.

Received: September 3, 2010
Published online: November 4, 2010

